



## Molecular Crystals and Liquid Crystals

Publication details, including instructions for authors and subscription information:

<http://www.tandfonline.com/loi/gmcl20>

### Impact of Contaminant Comonomers on the Various Conformational and Thermodynamic Properties of Poly (hydroxybenzoic acid) Liquid Crystals

Tarek M. Madkour<sup>a</sup>

<sup>a</sup> Department of Chemistry, Helwan University, Ain-Helwan, Cairo, Egypt

Version of record first published: 18 Oct 2010

To cite this article: Tarek M. Madkour (2002): Impact of Contaminant Comonomers on the Various Conformational and Thermodynamic Properties of Poly (hydroxybenzoic acid) Liquid Crystals, *Molecular Crystals and Liquid Crystals*, 373:1, 33-51

To link to this article: <http://dx.doi.org/10.1080/713738215>

PLEASE SCROLL DOWN FOR ARTICLE

Full terms and conditions of use: <http://www.tandfonline.com/page/terms-and-conditions>

This article may be used for research, teaching, and private study purposes. Any substantial or systematic reproduction, redistribution, reselling, loan, sub-licensing, systematic supply, or distribution in any form to anyone is expressly forbidden.

The publisher does not give any warranty express or implied or make any representation that the contents will be complete or accurate or up to date. The accuracy of any instructions, formulae, and drug doses should be independently verified with primary sources. The publisher shall not be liable for any loss, actions, claims, proceedings, demand, or costs or damages whatsoever or howsoever caused arising directly or indirectly in connection with or arising out of the use of this material.

# Impact of Contaminant Comonomers on the Various Conformational and Thermodynamic Properties of Poly(hydroxybenzoic acid) Liquid Crystals

TAREK M. MADKOUR

*Department of Chemistry, Helwan University, Ain-Helwan, Cairo, Egypt*

A conformational study of poly(hydroxybenzoic acid -co- hydroxynaphthoic acid) copolyesters was conducted to examine the effect of randomly positioning naphthoic units along the backbone of the poly(hydroxybenzoic acid) liquid crystals. This is usually done to bring down the processing temperature of the liquid crystal to practical working ranges. The COMPASS forcefield used throughout this study was developed particularly using *ab-initio* calculations to improve upon existing forcefields. Energy contour maps for both comonomers indicated a similar conformational behavior for the benzoic and naphthoic units. The radial distribution function calculated for the homopolymers and the copolyesters indicated a disruption of the short-range order in the copolyesters influenced by the greater length of the naphthoic units over that of the benzoic units. The important configurational properties such as the end-to-end distance and the radius of gyration show a linear dependence on the amount of the naphthoic units in the copolyester. Both the Kuhn segment parameters and the persistence length calculations indicate an increase in the stiffness of the chains with the increase in the amount of the naphthoic units. The Hildebrand solubility parameter evaluated from the cohesive energy densities of the copolyesters indicates, however, a constant value for the thermodynamic parameter across the entire compositional range of the copolyester.

**Keywords** Liquid crystals, conformational analysis, contour maps, Kuhn segment length, cohesive energy density, Hildebrand solubility parameter

## INTRODUCTION

The structures of poly(hydroxybenzoic acid) (PHBA) and poly(hydroxynaphthoic acid) (PHNA) have been of a great deal of interest to many scientific investigators for their close connection to the nature of the structural order in some of the commercially viable random copolyesters that show thermotropic liquid crystalline behavior [1]. These copolyesters

---

Received 7 May 2001; accepted 26 June 2001.

Address correspondence to Dr. Tarek M. Madkour, Department of Chemistry, Helwan University, Ain-Helwan, Cairo, Egypt, 11795. E-mail: drmadkour@yahoo.com

comprise mostly HBA groups (ca. 70%) plus one or two comonomer moieties to bring down the processing (flow) temperature to practical ranges. This is because the PHBA homopolymer is intractable and does not melt below temperatures at which degradation becomes a significant factor. Recently, Economy et al. [2] showed that PHBA exhibits two phase transitions at ca. 340°C and ca. 445°C, respectively, on the basis of differential scanning calorimetry (DSC) and thermomechanical analyzer (TMA) measurements. They concluded that the first transition at 340°C is either a crystal to a plastic crystal or to a high-order smectic phase transition and that the second transition at 445°C results in a nematic phase. The two phases of PHBA at room temperature were shown [3] to have the same space group  $Pbc2_1$  and to adopt the same conformation with glide symmetry along the chain. The two phenyls, constituting the c-axis repeat unit, are staggered by ca. 120°. Both orientations resulting from the disorder in the packing of the phenyl groups along the c-chain axis are present in the packing and the relative amount in the whole polymer sample is dependent on the synthesis procedure.

It was predicted by Chick et al. [4], using Monte Carlo models of the PHBA homopolymer, that a coarser microstructural scale results from the higher molecular axial ratios of molecules that are perfectly rigid and experience only steric interactions. On a molecular scale, however, Dannels and coworkers [5] showed that PHBA has a semiflexible molecular structure and therefore the molecular conformation was nonlinear. They indicated that the molecule is only considered straight over segmental lengths corresponding to the persistence length of PHBA. At 300°C, they determined that the persistence length is close to the contour length of 15 monomeric units. At contour lengths greater than that, they indicated that the semiflexibility of PHBA would become apparent.

2,6-Hydroxynaphthoic acid (HNA) has been, therefore, traditionally used as a comonomer with 1,4-hydroxybenzoic acid (HBA) as a means of disrupting crystallization and encouraging the formation of liquid crystalline mesophases. Hanna and Windle [6] observed a clear similarity between the two homopolymers of PHBA and PHNA. The main similarity between the two homopolymers is that both form high symmetry pseudohexagonal rotator phases. The  $a$  and  $b$  lattice parameters in the two rotator phases were very similar, which may explain why similar phases were observed across the entire compositional range of copolymers of both comonomers. They also reported a lower melting point for the PHNA as compared to that of PHBA homopolymer, which is probably due to the extra crankshaft type motion associated with the rotation of the side-step in the linked naphthoic ring [7].

The optimum range for the liquid crystals is brought down by decreasing the enthalpy of the system that is a result of inserting the modifying units at random positions along the chain, thus forming a random copolymer in which the crystallinity is frustrated without any additional loss of mesogenicity or reduction in the upper transition temperature. In addition, this also causes the entropy to rise as a result of the extra degrees of freedom within the mesophase, which helps in bringing down the processing temperature closer to an optimum range.

Since, as was shown, the bulk physical properties of liquid crystals depend to a great deal on the microstructure of the mesophases, i.e., the scale on which different levels of molecular order occur, it is vital that the conformational behavior of the individual molecules contributing to this order be evaluated and understood. It is the purpose of this work, therefore, to explore the conformational behavior of PHBA and PHNA homopolymers as well as the conformational behavior of their copolymers.

## SIMULATION METHODOLOGY

### Choice of Force Field

All calculations were performed with the molecular modeling package Insight II of Molecular Simulations Inc. (release 400) running on a Silicon Graphics Octane workstation. The quality of the forcefield, which consists of a set of analytical function terms and parameters and provides a detailed description of the inter- and intramolecular interactions as a function of the molecular structures and their relative positions, directly influences the reliability of the simulations to a great deal. The bulk simulation of the different polymer systems has been carried out using the COMPASS forcefield [8]. The COMPASS forcefield is a CFF-type forcefield [9] constructed using exact *ab-initio* quantum mechanics calculations. It was developed to improve upon existing forcefields. In the forcefield approach, the potential energy of a system is expressed as a sum of valence and nonbonded interactions:

$$\begin{aligned} E_{\text{total}} &= E_{\text{valence}} + E_{\text{nonbond}} \\ &= (E_{\text{bond}} + E_{\text{angle}} + E_{\text{torsion}} + E_{\text{inv}}) + (E_{\text{vdW}} + E_{\text{Coulomb}}) \end{aligned}$$

The valence terms parameterize the short-range intramolecular interactions that determine the bond lengths ( $E_{\text{bond}}$ ), bond angles ( $E_{\text{angle}}$ ), torsion angles ( $E_{\text{torsion}}$ ) and out-of-plane inversion angles ( $E_{\text{inv}}$ ). The nonbonded

interactions, which can be both intra- and intermolecular, are split into a dispersive van der Waals term ( $E_{\text{vdW}}$ ), and electrostatic term ( $E_{\text{Coulomb}}$ ). Other cross-terms are also important and well accounted for by the COMPASS forcefield.

## Energy Contour Maps

The energy contour maps for the homopolymers repeat units were calculated for ST and SR pairs of the dihedral angles T, S, and R as shown in Figures 1 and 2. Varying two torsions with respect to each other leads to a potential energy surface that is essential to understand the correlations between the various conformations of neighboring dihedral angles [10]. The energy surface was scanned every  $10^\circ$  from  $-180^\circ$  to  $+180^\circ$ . During the generation of the energy contour, the rest of the molecule was minimized by the conjugated gradient method until the energy derivatives were less than  $0.001 \text{ kcal mol}^{-1}$ . Torsion forcing of  $1000 \text{ kcal mol}^{-1}$  was used to force a torsion systematically to a grid of angles.

## Conformational Analysis

Various conformational properties of the two homopolymers and their copolyesters of different molar compositions were evaluated using RIS Metropolis Monte Carlo methods (RMMC) [11]. Unlike traditional rotational isomeric states methods, RMMC methods allows torsion angles to vary continuously and therefore do not impose the assumption of discrete rotational states. The method is thus based on relative energies of the new and the old conformation. The bond-based cutoff method was used for the simulations of the single polymeric chains in the  $\theta$ -condition. In this method, the parameters  $n_{\text{min}}$  and  $n_{\text{max}}$  affect the way van der Waals and Coulomb energies are evaluated in the RMMC simulation. The nonbond energies were not computed for atoms that are closer than  $n_{\text{min}}$  or further apart than  $n_{\text{max}}$ . The usual value for  $n_{\text{min}}$  was 3, whereas that of  $n_{\text{max}}$  was taken as 6 in order to include the interactions of the side chains of the neighboring repeat units in the energy evaluation.

RMMC simulations were done for polymers with 100 repeat units at room temperature. The number of the equilibration steps was 10,000 for each rotatable bond. This stage was necessary to bring the polymer chain from its initial conformation to a conformation typical for the chain in the melt at the desired temperature. The number of simulation steps was 50,000 steps for each rotatable bond. The block-averaged values of the mean

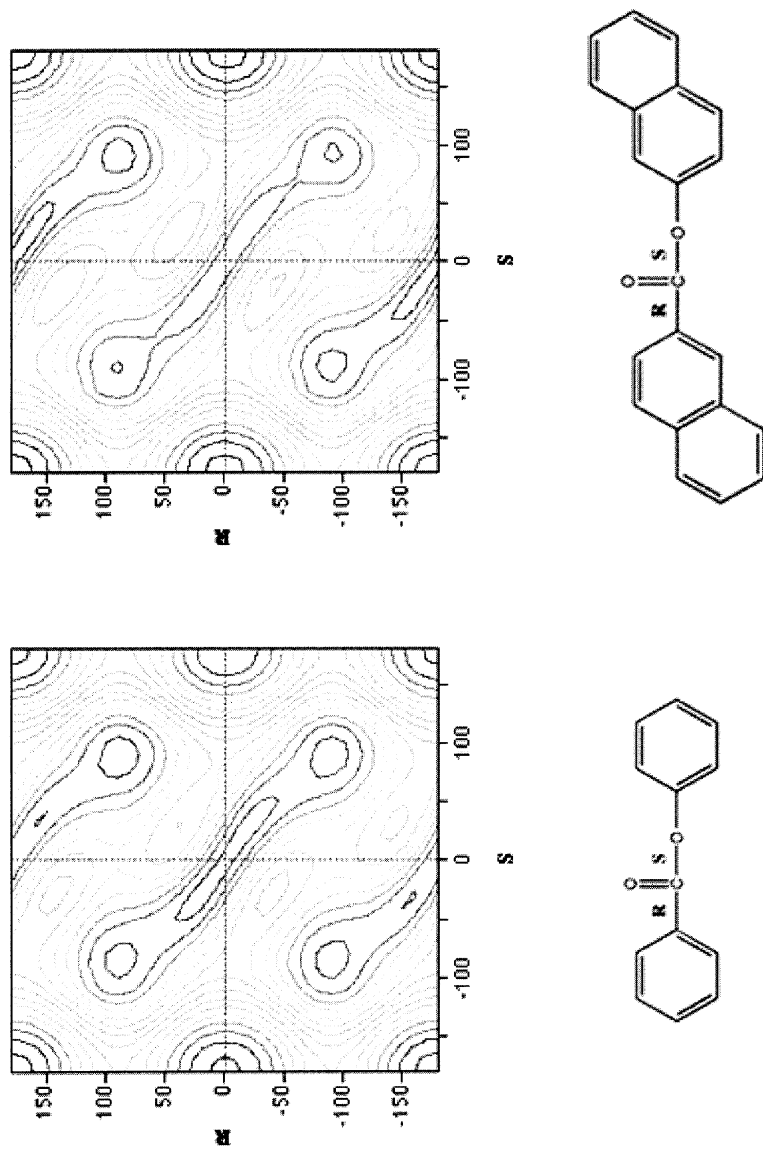


FIGURE 1 Energy contour maps displaying the potential energy as a function of rotation around torsional angles R and S.

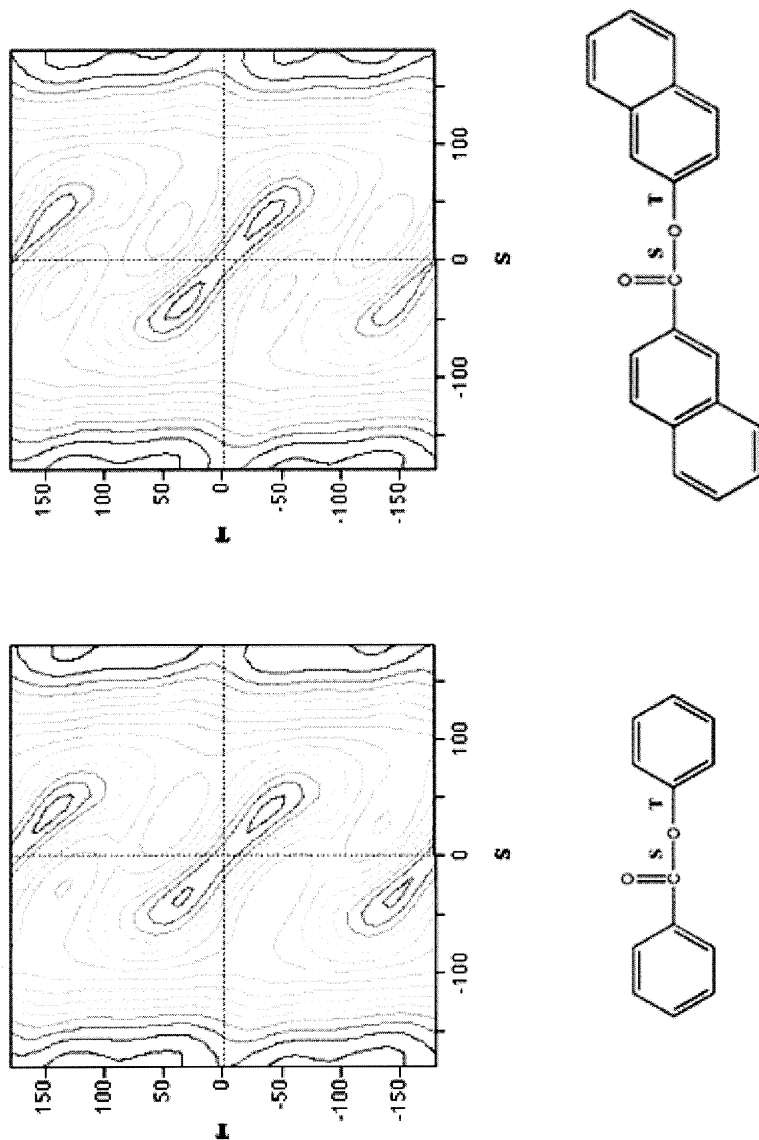


FIGURE 2 Energy contour maps displaying the potential energy as a function of rotation around torsional angles S and T.



squared end-to-end distance and energy were plotted as functions of the simulation step number in order to determine if the system was fully equilibrated. There was no evidence of any long-term drift in mean squared end-to-end distance and energy over the course of simulation, which indicated that the chains had reached a steady state. RMMC was used to calculate the conformational parameters such as the end-to-end distances, the radii of gyration and the persistence lengths as well as the Kuhn segment length and number of the entire compositional range.

## Bulk Simulations

The polymer structures were simulated in the bulk using three-dimensional cubic periodic boundary conditions to enable the molecular dynamics simulations to be carried out on relatively small molecular systems, in such a way that the atoms experience forces as if they were in the bulk phase [12]. The periodic replicates of the parent chain provide a simple method for introducing intermolecular interactions, necessary for the calculation of certain polymer properties, without increasing the number of atoms. In order to account for all of the long-range interactions, Ewald summation method was used to allow a charged particle to interact with all other particles in the simulation cell and with all of their images in an infinite array of periodic cells. Five chain conformations of each of the different polymers, consisting of 50 repeat units with full atomistic representations, were built using a traditional RIS method inside a cubic box with a volume that corresponds to the experimental density of the polymer at room temperature. After minimization, the systems were relaxed using molecular dynamics at 340°C, representing practical processing temperatures, for 1 ns at an average pressure of 0 atm. The velocity rescaling method was used in a constant particle number,  $N$ , volume, and temperature (NVT) ensemble. This was done to ensure the convergence of any of the high-energy initial configurations into more representative ones. The periodic boxes were then allowed to equilibrate under a NVT ensemble for another 1 ns at 25°C. A constant pressure, potential energy and total energy were observed during this equilibration stage. The data collection simulations were then performed at 25°C using NVT ensemble for 5 ns. This was chosen because of the known slow relaxation times for these polymers. At the end of every run, a trajectory file was stored for later analysis. Four runs were performed for each particular experiment for better averaging. The bulk simulations performed using the molecular dynamics techniques were used to evaluate the radial distribution function, the velocity autocorrelation function, the local

orientation function and the cohesive energy densities which were later used to estimate the Hildebrand solubility parameters.

## RESULTS AND DISCUSSION

Figures 1 and 2 display the energy contour maps for the HBA and HNA repeat units in case of rotations around R and S dihedral angles and around S and T dihedral angles, respectively. It is obvious from the figures that the extra phenylene group in the HNA repeat unit didn't influence the location of the local minima in both cases to a great deal. Therefore, it must be expected that the population of the trans and gauche states should be similar for both homopolymers.

The rotations around the S bond change the shape of the chain, which means the torsional behavior of the S bond is the most important from the viewpoints of liquid crystalline behavior and processability. The energy barrier height for rotation around the S bond was found to be more than  $12.1 \text{ kcal mol}^{-1}$ , implying that rotation is more restricted in this case than the one around the R bond, which was estimated to be of  $5.68 \text{ kcal mol}^{-1}$  in a good agreement with the experimental value [8] of  $5.3 \text{ kcal mol}^{-1}$ . Rotation around the S bond is probably difficult since it takes on some of the character of the adjacent double bond due to resonance. The ester linkage thus provides little opportunity for the chain to exhibit a configurational side step, as shown in the figures [7]. In fact, it was reported [13] that ester links are often used in small molecule liquid crystals, where its tendency to promote mesogenicity is ranked above that of a single bond linking the adjacent phenyl groups. The conformational energy calculations indicate that the phenylene group attached through the T bond is prevented from rotating into the same plane of the ester by steric interaction between one of the ortho hydrogen atoms on the phenyl ring and the carbonyl oxygen atom. The side step associated with the ester provides an additional measure of conformational freedom in the liquid crystalline phase through crankshaft type motions associated with rotations around R and T bonds, causing the second phenyl group to move laterally with respect to the first.

### Radial Distribution Function and Velocity Autocorrelation Function

The radial distribution function gives a measure of the probability that, given the presence of an atom at the origin of an arbitrary reference frame, there will be an atom with its center located in a spherical shell of

infinitesimal thickness at a distance  $r$  from the reference atom. The radial distribution function,  $g_{\alpha\beta}(r)$ , is calculated from the average of the static relationship of every given pair of particles,  $\alpha\beta$ , as [14]

$$g_{\alpha\beta}(r) = \frac{\langle n_{\alpha\beta}(r) \rangle}{4\pi r^2 \Delta r \rho_{\alpha\beta}}, \quad (1)$$

where  $\langle n_{\alpha\beta}(r) \rangle$  is the average number of atom pairs in the spherical shell between  $r$  and  $r + \Delta r$ ,  $\alpha\beta$  denotes the possibility that  $\alpha$  and  $\beta$  particles may be of a different chemical nature, and  $\rho_{\alpha\beta}$  is the density of atom pairs of type  $\alpha\beta$ . By investigating the radial distribution function, more information on the local packing influenced by specific interactions could be obtained. The radial distribution functions of poly(hydroxybenzoic acid), poly(hydroxynaphthoic acid), and poly(HBA-co-HNA) copolyester of 50/50 molar composition obtained from the molecular dynamics studies of bulk polymers are depicted in Figure 3. The figure illustrates the short-range order in case of the homopolymers resulting from the relatively rigid bond lengths and angles and the weak spatial correlation among particles at large topological distances. More interestingly, close inspection of the radial distribution function of the copolymer reveals the disruption of the short-range order resulting from randomly positioning the naphthoic units along the backbone of the poly(hydroxybenzoic acid) chains as influenced by the greater length of the naphthoic units over that of the benzoic units. Even though melting points are determined by competing factors such as statistical considerations [15] and nonperiodic lattice formation [16], this disruption will most probably influence the crystallinity of the chains, causing its melting point to decrease to proper working ranges without any expected reduction in the stability of the mesophases since both monomeric units are mesogenic in nature.

Figure 4 represents the velocity autocorrelation functions of the PHBA, PHNA, and (HBA-co-HNA) copolyester obtained from the molecular dynamics studies of bulk polymers. The copolyester has a molar ratio equal to that of the two comonomers. Of interest here is the effect of the molecular structure on the dynamic and vibrational properties of the materials at the elevated temperatures of 340°C common during the processing of these materials. The velocity autocorrelation function,  $C$ , is defined as [12]:

$$C(m) = \frac{1}{n} \sum_{i=1}^n V(m+i) \times V(i), \quad (2)$$

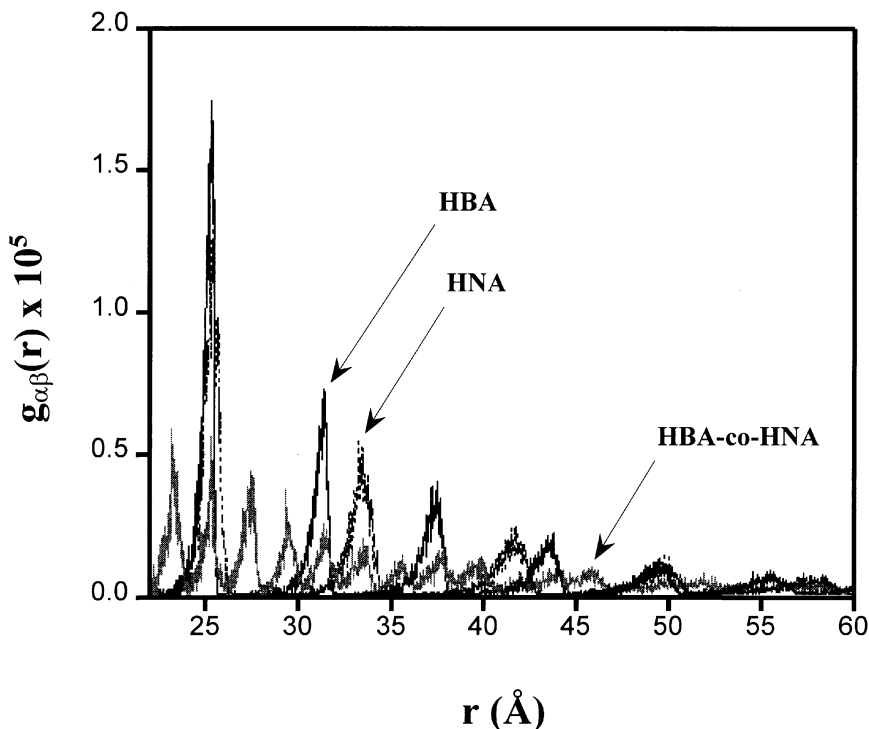


FIGURE 3 Comparison of the pair radial distribution functions of PHBA, PHNA, and (HBA-co-HNA) copolyester. The copolyester has a molar ratio equal to that of the two comonomers.

where  $m$  is the minimum number of points allowed during the calculations,  $n$  is the number of data points used for averaging and  $V$  is the velocity of a particle  $i$ . It is obvious from the figure that the added degree of freedom due to randomly positioning the naphthoic units in the copolymer did not have much influence on the dynamics of the systems, which indicates that the effect of the copolymerization is rather static, or conformational, than dynamic.

### Local Orientation Function

The correlation between the orientations of the phenyl rings was studied using the orientation function,  $p_2$ , defined in terms of second order Legendre polynomials describing the ensemble average of an angle made by a section of the polymer chain with a specified direction.  $p_2(\cos \theta)$  is given by [17]

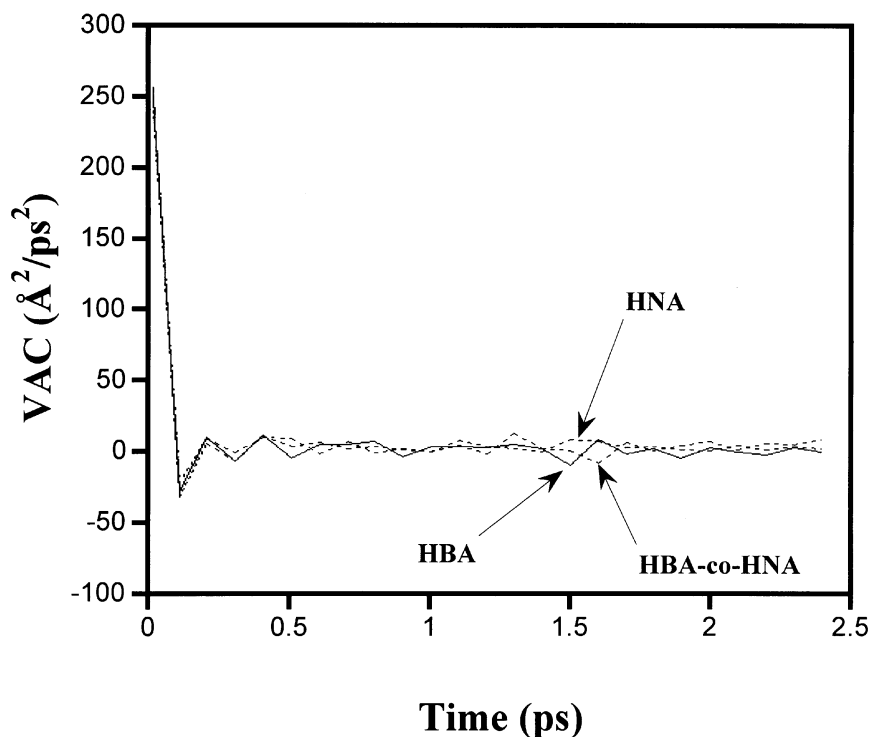


FIGURE 4 Effect of the molecular structure on the velocity autocorrelation function of PHBA, PHNA, and (HBA-co-HNA) copolyester. The copolyester has a molar ratio equal to that of the two comonomers.

$$p_2(\cos \theta) = \frac{1}{2}[3\langle \cos^2 \theta \rangle - 1], \quad (3)$$

where  $\theta$  is the angle between any two vectors  $i$  and  $j$  defining the normals of two phenyl groups.  $\langle \dots \rangle$  denotes the average of all vector pairs having an angle  $\theta$  with respect to each other. Figure 5 shows a plot of  $p_2(\cos \theta)$  as a function of  $\theta$  angle obtained from the molecular dynamics studies of both homopolymers in the bulk state. Similar to the observation made by the energy contour maps, both homopolymers showed a similar orientational behavior. No comparison was made with the copolymer because alignment studies are only possible for homopolymers. The correlation functions show a strong tendency for parallel alignment at angles greater than  $80^\circ$ , possibly due to near-neighbor interaction correlations, caused by the strong steric repulsions among the phenyl rings, which is such that the normals of the phenyl rings tend to be parallel to each other.

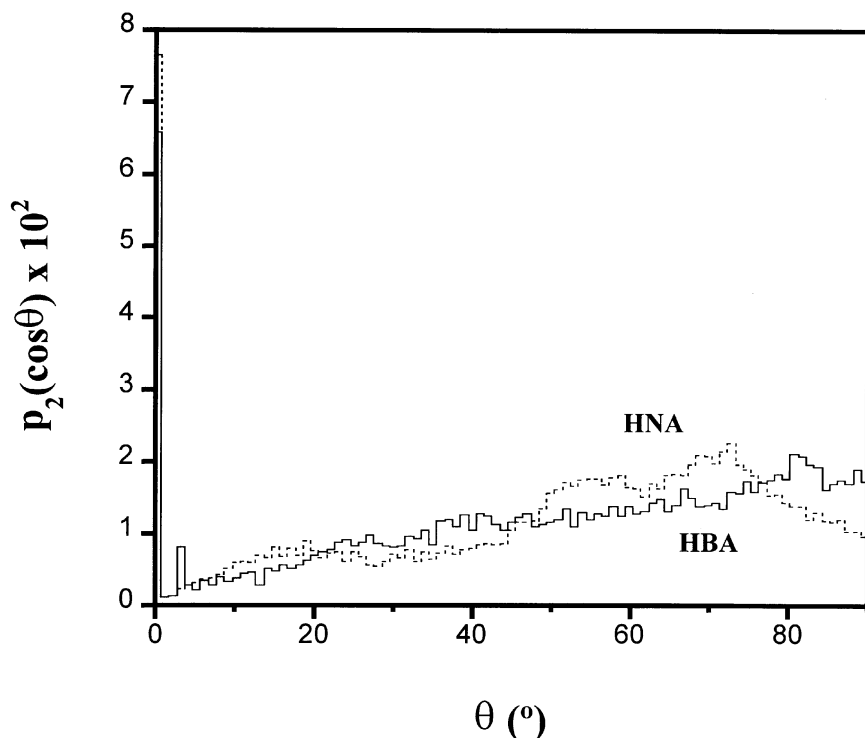


FIGURE 5 Comparison of the local orientation functions of PHBA and PHNA.

### Conformational Analysis

To examine the possible effect of randomly positioning naphthoic units in the copolyesters chain backbone, the conformational properties such as the end-to-end distance, the radius of gyration, and the persistence length were evaluated as a function of the molar composition of (HBA-co-HNA) copolyesters. Error bars shown in all the figures are referring to the standard errors. The end-to-end distance,  $r$ , of a single chain is defined as [18]

$$r = \sum_{i=1}^n l_i, \quad (4)$$

where  $l_i$  denotes the vector along backbone bond  $i$ , and  $n$  denotes the number of backbone bonds in the molecule. The radius of gyration,  $S$ , is defined as the root mean squared distance of the atoms in the molecule from their common center of mass and is given by [19]

$$S^2 = \frac{\sum_{i=1}^N m_i S_i^2}{\sum_{i=1}^N m_i}, \quad (5)$$

where  $S_i$  denotes the distance of atom  $i$  from the center of mass, and  $N$  denotes the total number of atoms. Figures 6 and 7 illustrate the dependence of the mean squared end-to-end distance and radius of gyration on the molar composition of the naphthoic units in (HBA-co-HNA) copolyesters,  $\Phi_{\text{HNA}}$ .

Figure 8 illustrates the dependence of the persistence length on the molar composition of the naphthoic acid in the copolyester. The persistence length is a universal measure of the polymer chain stiffness. It is defined as the average distance traversed by the chain backbone along its initial direction before the chain loses “memory” of this direction. Mathematically, the persistence length,  $\langle q_1 \rangle$ , can be defined as the mean projection of the

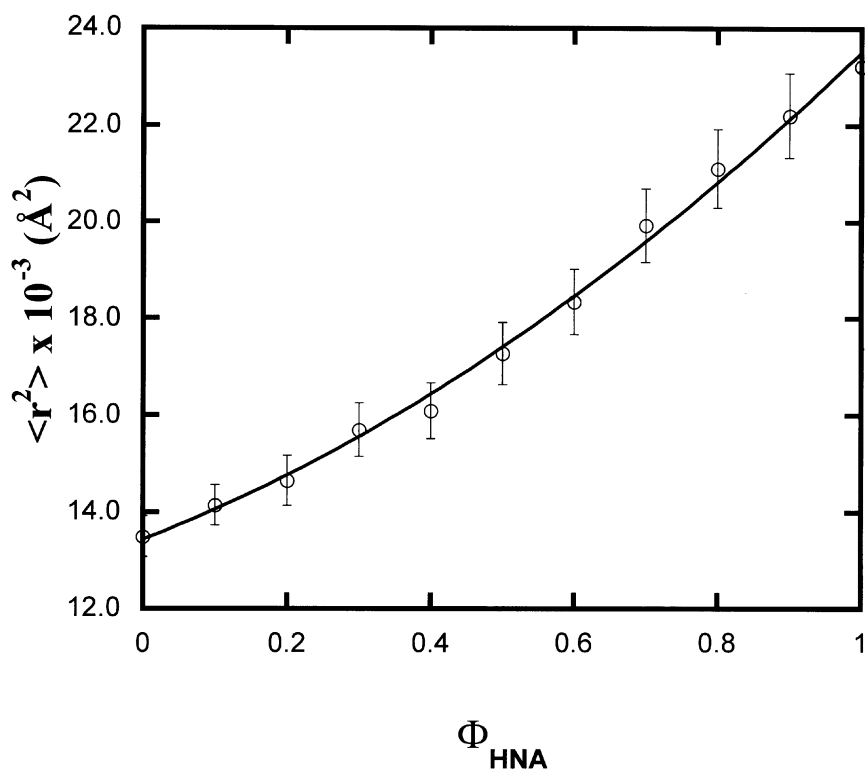


FIGURE 6 The dependence of the root-mean-squared end-to-end distance on the mole fraction of the naphthoic units in the (HBA-co-HNA) copolyesters.

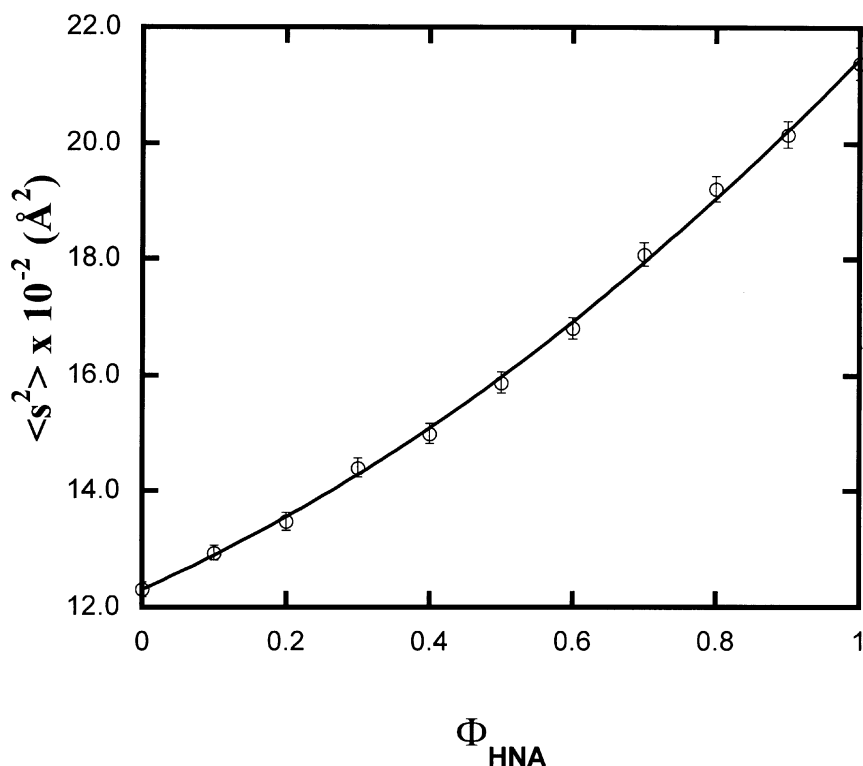


FIGURE 7 The dependence of the root-mean-squared radius of gyration on the mole fraction of the naphthoic units in the (HBA-co-HNA) copolyesters.

end-to-end vector on the first bond of the chain. An alternative definition,  $\langle q_2 \rangle$ , is the mean projection of all subsequent bond vectors on a bond in the chain backbone, averaged over all bonds between the two chain ends. Both of these quantities are investigated in Figure 8. It is obvious that the values of the persistence length are consistent throughout the chains because the averaging over all bonds did not bring any improvement over the sampling of the measured parameter. This is due to the rigidity of the polymeric rods. Furthermore, the increase in the persistence length as a function of the molar composition of the naphthoic units is moderate if compared to that of the end-to-end distance or the radius of gyration, thus indicating the high stiffness of the polymeric chains at all compositions.

To further quantify the effect of adding more naphthoic units in the backbone of the copolyester on the stiffness of the chains, it is appropriate to consider the Gaussian chain parameters such as the number of Kuhn



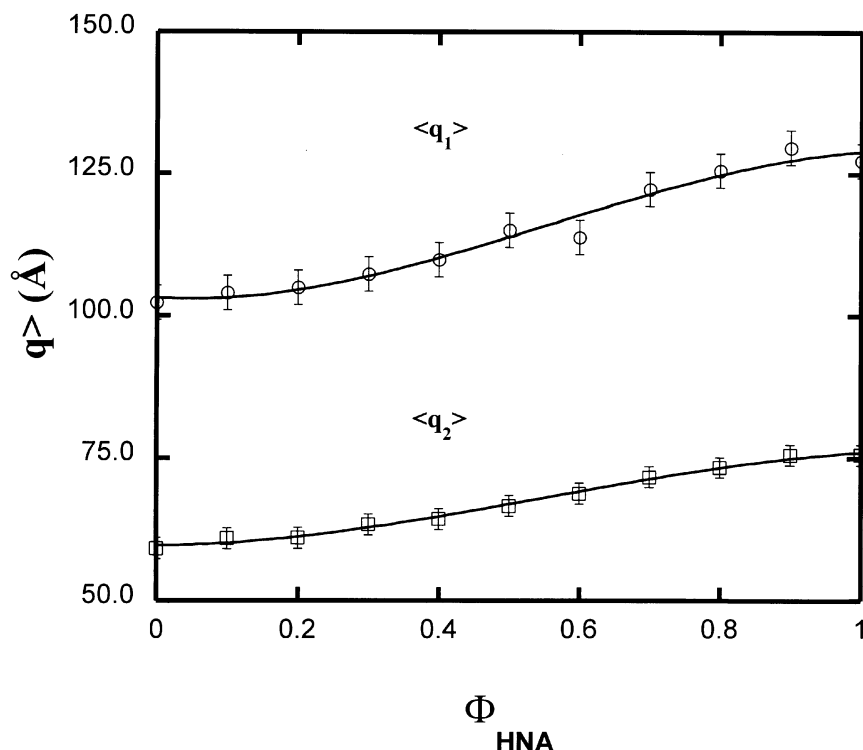


FIGURE 8 The dependence of the average persistence length on the mole fraction of the naphthoic units in the (HBA-co-HNA) copolyesters.

segments and the Kuhn segment length. The fully extended chain length,  $R_{\max}$ , for a Gaussian chain is given by the product of the number of segments,  $N$ , and the segment length,  $b$ . The mean squared end-to-end distance for a Gaussian chain,  $\langle R^2 \rangle$ , is given by the product of the number of segments and the square of the segment length [19]

$$R_{\max} = Nb, \quad (6a)$$

$$\langle R^2 \rangle = Nb^2. \quad (6b)$$

Assuming that the copolyester chain could be treated as both a Gaussian chain and as a molecular chain,  $N$  and  $b$  could therefore be calculated using the values for the fully extended length and the mean squared end-to-end distance evaluated using the RMMC techniques. Table 1 lists the values of the Gaussian chain parameters as a function of increasing the mole fraction

TABLE 1 Evaluation of the Gaussian chain parameters

$\Phi_{HNA}^a$	$R_{max}^b (\text{\AA})$	$\langle r^2 \rangle^c (\text{\AA}^2)$	$b^d (\text{\AA})$	$N^e$
0.0	128.64	13492	104.89	1.23
0.1	130.54	14139	108.31	1.21
0.2	134.33	14646	109.03	1.23
0.3	138.13	15740	113.95	1.21
0.4	140.02	16187	115.60	1.21
0.5	143.82	17277	120.13	1.20
0.6	147.61	18340	124.25	1.19
0.7	153.30	19934	130.03	1.18
0.8	157.10	21108	134.36	1.17
0.9	160.90	22205	138.01	1.17
1.0	166.58	23226	139.43	1.20

<sup>a</sup>The mole fraction of the naphthoic units in the (HBA-co-HNA) copolyesters.

<sup>b</sup>The fully extended length of the copolyester chains.

<sup>c</sup>The mean squared end-to-end distance calculated using RMMC.

<sup>d</sup>The Kuhn segment length.

<sup>e</sup>The number of Kuhn segments per copolyester chain.

of the naphthoic units in the polymeric chains. If a polymer molecule is extremely stiff, it will probably consist of only one Kuhn segment whose length is the length of the whole molecule. Alternatively, if the polymer chain is flexible enough, it will consist of many short Kuhn segments of much smaller length. Therefore, it must be obvious from the table that the incorporation of the naphthoic units into the copolymeric chain causes the number of the Kuhn segments to decrease and the Kuhn segment length to increase, indicating the increased stiffness of the copolyester chains by adding more naphthoic units into the polymeric chains.

### Cohesive Energy Density and Hildebrand Solubility Parameter

To complete this study, it is vital to investigate the influence of the added naphthoic units on the Hildebrand solubility parameter of the copolyester. The cohesive energy,  $E_{coh}$ , of a polymer in the bulk can be defined as the increase in energy per mole of substance if all intermolecular forces are eliminated [14]. Using our molecular dynamics investigation,  $E_{coh}$  could be estimated by the difference in the potential energies between the parent chain in the bulk and the parent chain in vacuum, i.e.,

$$E_{coh} = E_{isolated} - E_{bulk}. \quad (7)$$

The Hildebrand solubility parameter ( $\delta$ ) can be obtained from the cohesive energy density as

$$\delta = \left( \frac{E_{coh}}{V} \right)^{1/2}, \quad (8)$$

TABLE 2 Hildebrand solubility parameters and the melting points [7] for various (HBA-co-HNA) copolyesters with different molar compositions

$\Phi_{HNA}$	$\delta$ (J/cc) <sup>1/2</sup>	$T_m$ (°C)
0.0	21.58	—
0.1	22.82	—
0.2	24.01	340
0.3	22.80	—
0.4	22.12	250
0.5	23.14	—
0.6	23.06	275
0.7	22.70	—
0.8	22.88	310
0.9	23.44	—
1.0	23.67	—

where  $V$  is the volume of the amorphous cell. Table 2 lists the values of the Hildebrand solubility parameter for a series of (HBA-co-HNA) copolyesters with increasing content of the naphthoic units. For the purpose of comparison, some values for the melting points of copolyesters of different compositions are also reported [7]. It is clear from the table that the Hildebrand solubility parameter remained fairly constant for the whole series of the copolyesters. This is due to the expected similar values for the intermolecular forces in both cases of the comonomeric units. However, the values for the melting point have gone through a minimum near the 50/50 ratio, implying that the melting behavior of the copolyester depends to a great deal on the local molecular packing rather than on the intermolecular forces between the polymeric chains.

## CONCLUSION

Traditionally, comonomeric units of 2,6-hydroxynaphthoic acid are used to bring down the processing temperature of the poly(hydroxybenzoic acid) to practical ranges by disrupting its crystallinity. To examine the effect of the copolymerization on the conformational behavior of the polymers influencing the final bulk properties of the liquid crystals, RMMC and molecular dynamics techniques were used. It was shown that rotations around the bond linking the carbonyl carbon and the ester oxygen are more restricted than other rotations. This is important since these rotations are the ones responsible for the change in the shape of the chains. Energy contour maps generated for both comonomeric units indicated similar conformational behavior for both comonomers. Other predicted similarities for the

homopolymers were based on their solubility parameters, radial distribution function, and their velocity autocorrelation function. This is in line with the observation that both homopolymers form high symmetry pseudohexagonal rotator phases with the  $a$  and  $b$  lattice parameters in both cases are very similar. However, the behavior of the copolyesters was predicted to be of a different nature resulting from the disruption of the short-range order in the poly(hydroxybenzoic acid) chains as influenced by the greater length of the naphthoic units over that of the benzoic units. Configurational properties such as the end-to-end distance, the radius of gyration, and the persistence length show a linear dependence on the amount of the naphthoic units in the copolyester. Both the Kuhn segment parameters and the persistence length indicate an increase in the stiffness of the chains with the increase of the naphthoic units amount. The Hildebrand solubility parameter evaluated from the cohesive energy densities of the copolyesters indicates, however, a constant value for the thermodynamic parameter across the entire compositional range of the copolyester. This is probably due to the expected similar values for the intermolecular forces in both cases of the comonomeric units. However, the values for the melting point have gone through a minimum near the 50/50 ratio, implying that the melting behavior of the copolyester depends to a great deal on the local molecular packing rather than on the intermolecular forces between the polymeric chains.

## REFERENCES

1. T. M. Madkour, in *Polymer data handbook*, J. E. Mark, ed. (Oxford University Press, New York, 1999), pp. 583–585.
2. J. Economy, W. Volksen, C. Viney, R. Geiss, R. Siemens, and T. Karis, *Macromolecules* 21, 2777 (1988).
3. P. Iannelli and D. Y. Yoon, *J. Polym. Sci. Polym. Phys. Ed.*, 33, 977 (1995).
4. L. A. Chick, C. Viney, and I. A. Aksay, Liquid crystal-like phase separation in systems of macroscopic rods. In *Processing Science of Advanced Ceramics*, I. A. Aksay, G. L. McVay and D. R. Ulrich, eds. (Materials Research Society, Pittsburgh, PA, 1989), pp. 331–342.
5. C. M. Dannels, C. Viney, R. J. Twieg, and M. Y. Chang, *Mol. Cryst. Liq. Cryst.* 198, 341 (1991).
6. S. Hanna and A. H. Windle, *Polymer* 33, 2825 (1992).
7. A. M. Donald and A. H. Windle, *Liquid Crystalline Polymers* (Cambridge University Press, Cambridge, 1992).
8. H. Sun, *J. Phys. Chem.* 102, 7338 (1998).
9. D. Rigby, H. Sun, and B. E. Eichinger, *Polym. Int.* 44, 311 (1997).
10. T. Launne, I. Neelov, and F. Sundholm, *Polymer* 40, 2313 (1999).
11. J. D. Honeycutt, *Comput. Theor. Polym. Sci.* 8, 1 (1998).
12. T. M. Madkour and A. M. Barakat, *Comput. Theor. Polym. Sci.* 7, 35 (1997).
13. R. A. Vora, N. Dixit, G. D. Karadkar, and R. G. Patel, *Mol. Cryst. Liq. Cryst.*, 108, 187 (1984).

14. W.-K. Kim and W. L. Mattice, *Comput. Theor. Polym. Sci.* 8, 353 (1998).
15. P. J. Flory, *J. Chem. Phys.* 15, 684 (1947).
16. A. H. Windle, C. Viney, R. Golombok, A. M. Donald, and G. R. Mitchell, *Faraday Discuss. Chem. Soc.* 79, 55 (1985).
17. R. Khare and M. E. Paulaitis, *Macromolecules* 26, 7203 (1993).
18. T. M. Madkour, O. M. Ibrahim, and A. H. Ebaid, *Comput. Theor. Polym. Sci.* 10, 15 (2000).
19. P. J. Flory, *Principles of Polymer Chemistry* (Cornell University Press, Ithaca, NY, 1953).